

# g-C<sub>3</sub>N<sub>4</sub> Photocatalyzed Decarboxylative Oxidation of Carboxylic Acids and the Oxidation of Alkenes and Alkanes

Sangita Bishi,<sup>a, b, c</sup> Bhabani Sankar Lenka,<sup>b</sup> Peter Kreitmeier,<sup>c</sup> Oliver Reiser,<sup>c,\*</sup> and Debayan Sarkar<sup>b,\*</sup>

<sup>a</sup> Department of Chemistry, National Institute of Technology, Rourkela, 769008, India

<sup>b</sup> Department of Chemistry, Indian Institute of Technology, Indore, Madhya Pradesh 453552, India  
E-mail: sarkard@iiti.ac.in

<sup>c</sup> Institut für Organische Chemie, Universität Regensburg, Regensburg, Bavaria 93053, Germany  
E-mail: oliver.reiser@chemie.uni-regensburg.de

Manuscript received: January 30, 2024; Revised manuscript received: June 5, 2024;

Version of record online: July 22, 2024



Supporting information for this article is available on the WWW under <https://doi.org/10.1002/adsc.202400117>

© 2024 The Author(s). Advanced Synthesis & Catalysis published by Wiley-VCH GmbH. This is an open access article under the terms of the Creative Commons Attribution License, which permits use, distribution and reproduction in any medium, provided the original work is properly cited.

**Abstract:** The decarboxylative oxygenation of readily available carboxylic acids as well as the oxidation of alkenes and alkanes has been accomplished through visible light using g-C<sub>3</sub>N<sub>4</sub> as a robust and recyclable catalyst. The scalable protocol furnishes an array of aldehydes and ketones under mild reaction conditions, requiring only molecular oxygen as an oxidant. Notably, no addition of stoichiometric amounts of base is required, and furthermore, the reaction proceeds efficiently open to the air.

**Keywords:** Photo redox catalysis; Oxidation; Graphitic carbonitride (g-C<sub>3</sub>N<sub>4</sub>); Carbonyl compounds

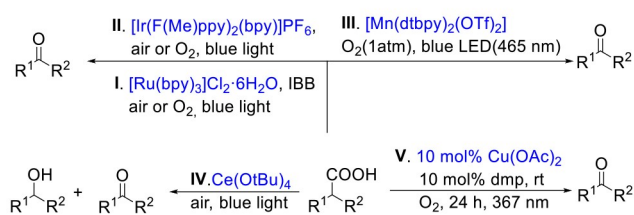
Organic scaffolds containing carbonyl moieties (e.g. aldehydes and ketones) are essential for synthetic organic chemistry in academia and industry. In the modern chemical industry, transformations employing molecular oxygen are attractive processes from an economic and environmental point of view; this becomes even more valuable when the transformation is augmented with non-metallic heterogeneous catalysts as this circumvents post-reaction metallic contamination. New catalytic protocols employing visible light have been prominent in minimizing waste-forming reactions. However, further improvements call for photocatalyst regeneration and benign terminal oxidants or reductants. Thus, heterogeneous non-

metal-based photocatalysts are essential for attaining sustainability in organic transformations. The oxidation of hydrocarbons and alcohols<sup>[1–6]</sup> has been the primary source for the generation of carbonyls, while the corresponding reduction of carboxylic acids is generally characterized by stoichiometric employment of hydride reagents.

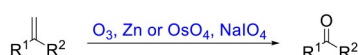
More recently, the decarboxylative oxygenation that allows the generation of aldehydes or ketones from carboxylic acids with a loss of one carbon unit has found broad interest, given that carboxylic acids are a versatile and abundant feedstock. Both thermal and especially relevant for this study photochemical protocols have been developed for this transformation.<sup>[7,8,17,9–16]</sup> Apart from carboxylic acids, alkenes<sup>[3,18–23]</sup> (Scheme 1Ab) and alkanes<sup>[3,24–27]</sup> (Scheme 1Ac) can also be converted to carbonyl compounds by C,C-double bond cleavage or C<sub>sp</sub>3–H activation. Despite significant advances, the development of an inexpensive and recyclable photocatalytic system for such transformations is still desirable. Rueping and co-workers reported related findings to our study, employing mesoporous graphene nitride (mpg-CN)<sup>[28]</sup> (Scheme 1Ad).<sup>[29]</sup> Although, g-C<sub>3</sub>N<sub>4</sub> is considered to have some drawbacks over mpg-CN such as a lower surface area, nitrogen density, or less availability of the surface for functionalization and catalytic applications,<sup>[28]</sup> herein, we report a protocol for employing heterogeneous graphitic carbon nitride (g-C<sub>3</sub>N<sub>4</sub>) as photocatalyst.<sup>[30–36]</sup> We find g-C<sub>3</sub>N<sub>4</sub> to be advantageous for the title reaction concerning activity

A. Previous work

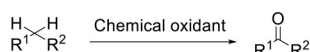
a. Homogeneous decarboxylative oxygenation



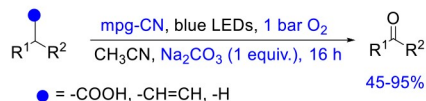
b. Approach for C=C bond cleavage



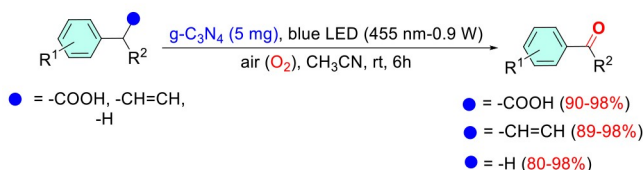
c. Approach for oxidation of C(sp<sup>3</sup>)-H bond



d. Heterogeneous photo-oxygenation



B. This Work



**Scheme 1.** Strategies for synthesis of carbonyl compounds. A(a) Decarboxylative oxygenation of carboxylic acids. A(b) Oxidative cleavage of olefins. A(c) Oxidation of C(sp<sup>3</sup>)-H bond to carbonyl compounds. A(d) Photo-oxygenation by heterogeneous photocatalyst. B. Our approach: Photooxygenation by g-C<sub>3</sub>N<sub>4</sub> photocatalyst.

and reaction time as well as not having to rely on stoichiometric bases as additives.

Both, mpg-CN<sup>[37]</sup> used in the previous study<sup>[29]</sup> and g-C<sub>3</sub>N<sub>4</sub><sup>[30,36]</sup> used here have been prepared by protocols reported in the literature, which also contain characterization detailed data (see also the SI for XRD and Tauc plot data obtained by us for g-C<sub>3</sub>N<sub>4</sub>). We attribute the higher photocatalytic activity of g-C<sub>3</sub>N<sub>4</sub> compared to mpg-CN to the high crystallinity of the former.<sup>[38,39]</sup>

We began our investigation by subjecting 4-methoxyphenylacetic acid (**1d**) to irradiation in the presence of photocatalyst g-C<sub>3</sub>N<sub>4</sub> (Table 1 and Figure 1a,b; see also SI, Scheme S1 for synthetic methods). We were pleased to find that under an air atmosphere, 4-methoxy benzaldehyde (**2d**) could be obtained in up to

**Table 1.** Screening of decarboxylative oxygenation of 4-methoxyphenylacetic acid.<sup>[a]</sup>

Entry	PC	Solvents	Light conditions	Yield <sup>[b]</sup> (%)
1	g-C <sub>3</sub> N <sub>4</sub>	CH <sub>3</sub> CN	Blue	94
2 <sup>[c]</sup>	g-C <sub>3</sub> N <sub>4</sub>	CH <sub>3</sub> CN	Blue	94
3 <sup>[d]</sup>	–	CH <sub>3</sub> CN	Blue	0
4	g-C <sub>3</sub> N <sub>4</sub>	CH <sub>3</sub> CN	Dark	0
5	g-C <sub>3</sub> N <sub>4</sub>	THF	Blue	31
6	g-C <sub>3</sub> N <sub>4</sub>	EtOH	Blue	40
7	g-C <sub>3</sub> N <sub>4</sub>	DCE	Blue	50
8	g-C <sub>3</sub> N <sub>4</sub>	Acetone	Blue	50
9	g-C <sub>3</sub> N <sub>4</sub>	Hexane	Blue	30
10	g-C <sub>3</sub> N <sub>4</sub>	DMSO	Blue	20
11	g-C <sub>3</sub> N <sub>4</sub>	DCM	Blue	45
12	g-C <sub>3</sub> N <sub>4</sub>	H <sub>2</sub> O	Blue	10
13 <sup>[e]</sup>	g-C <sub>3</sub> N <sub>4</sub>	CH <sub>3</sub> CN	Blue	0
14 <sup>[f]</sup>	g-C <sub>3</sub> N <sub>4</sub>	CH <sub>3</sub> CN	Blue	0
15	g-C <sub>3</sub> N <sub>4</sub>	CH <sub>3</sub> CN	Green	30
16	g-C <sub>3</sub> N <sub>4</sub>	CH <sub>3</sub> CN	Red	5
17	TiO <sub>2</sub>	CH <sub>3</sub> CN	Blue	10
18	CdS	CH <sub>3</sub> CN	Blue	5
19 <sup>[g]</sup>	g-C <sub>3</sub> N <sub>4</sub>	CH <sub>3</sub> CN	Blue	94
20	g-C <sub>3</sub> N <sub>4</sub>	CH <sub>3</sub> CN/H <sub>2</sub> O (1:1)	Blue	94

<sup>[a]</sup> Reaction conditions: **1d** (0.1 mmol), PC (5 mg), Solvents (3 mL), 6 h, air, LED light (1 W), rt.

<sup>[b]</sup> Yields determined by <sup>1</sup>H NMR analysis.

<sup>[c]</sup> LED light (3 W).

<sup>[d]</sup> No catalyst.

<sup>[e]</sup> N<sub>2</sub> balloon.

<sup>[f]</sup> Ar balloon.

<sup>[g]</sup> O<sub>2</sub> balloon.

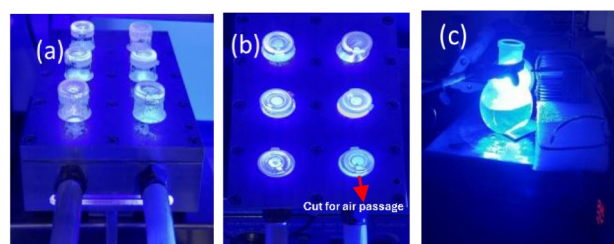


**Figure 1.** (a) and (b) Setup for small scale synthesis under irradiation of 0.9 W blue LED, and (c) Gram-scale reaction setup for 4-methoxy phenylacetic acid under irradiation of 1 W Kessil blue LED light.

94% yield (Table 1, entry 1). Blue light (455 nm) irradiation and acetonitrile were found to be optimal. Moreover, other heterogeneous photocatalysts such as

TiO<sub>2</sub> or CdS or omission of g-C<sub>3</sub>N<sub>4</sub> did not promote the transformation to a significant extent. Notably, the procedure employed does not require a base, contrasting the recent report by Rueping et al. which mandates 1 equiv. of Na<sub>2</sub>CO<sub>3</sub> as an additive.<sup>[29]</sup> Moreover, air rather than oxygen proved to be sufficient for achieving high yields in short reaction times.

Under the optimized conditions, a variety of phenylacetic acids bearing electron-withdrawing or electron-donating groups on the phenyl ring were utilized, affording the desired aldehyde products **2a–2v** in high yields (Table 2). Likewise, heteroaryl acetic acids bearing a thiophene, furan, pyridine, or indole moiety (**2w–2aa**) proved to be excellent substrates for the title transformation (Table 2).

Secondary phenylacetic acids are also efficiently converted to the corresponding ketones under standard conditions (Table 3). Late-stage functionalization of drug molecules (e. g., ibuprofen, flurbiprofen, naproxen, ketoprofen, isoxepac, zaltoprofen etc.) containing a phenylacetic acid moiety was also successfully carried out, affording the corresponding aldehydes or ketones (Table 3).

Besides benzylic, allylic carboxylic acid **3e** also gave rise to the corresponding ketone in high yield (Table 3). In line with Rueping's study,<sup>[29]</sup> aliphatic carboxylic acids failed in the title transformation (see SI, Scheme S2).

Apart from aldehydes and ketones, amides can also be obtained from the corresponding N-substituted  $\alpha$ -amino acids (**4f**) (Table 3).

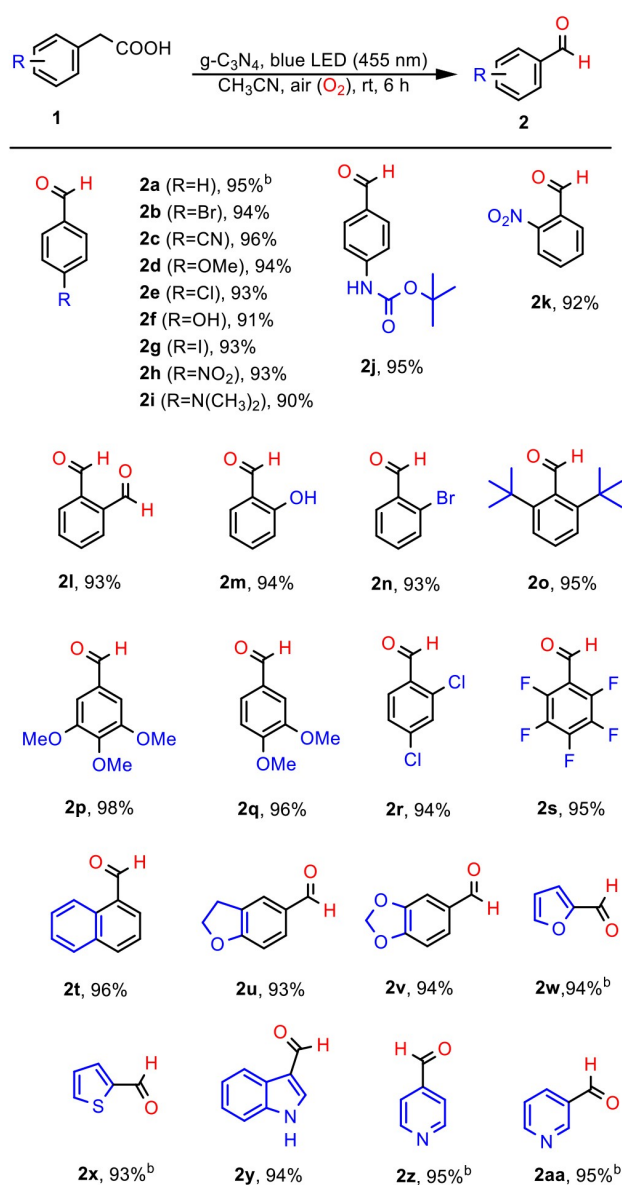
Scale-up was demonstrated for the transformation of 4-methoxyphenylacetic acid (**1d**, 30 mmol) to afford 4-methoxybenzaldehyde (**2d**) with excellent yield (Scheme 2, Figure 1c). Notably, only 5 mg of g-C<sub>3</sub>N<sub>4</sub> was still needed without prolonging the reaction time for the process.

Next, we applied the methodology to the oxidative cleavage of vinyl arenes and the oxidation of benzylic alkanes (Tables 4 and 5), which also proceeded in high yields and short reaction times.

To further investigate the practicability of the protocol, a recycling experiment was performed (Figure 2). g-C<sub>3</sub>N<sub>4</sub> was recovered by centrifugation after the reaction and reused in 7 cycles without significant loss in catalytic activity. The characterization data of the recovered g-C<sub>3</sub>N<sub>4</sub> i. e., XRD (Figure 3a), FTIR (Figure 3b), UV-vis DRS (Figure 3c), FESEM (Figure 3d,e) images of fresh and recovered g-C<sub>3</sub>N<sub>4</sub> and EDS (Figure 3f,g) analysis clearly shows robustness, stability, and durability of this heterogeneous photocatalyst.<sup>[39]</sup>

Several control experiments were performed using 4-methoxy phenylacetic acid (**1d**) to confirm the mechanism of the reaction. Under N<sub>2</sub> atmosphere and using anhydrous acetonitrile, the desired product **2d** was not detected, which confirms the involvement of

**Table 2.** Scope of mono-, di- and tri-substituted aryl acetic acids and heteroaryl acetic acids for decarboxylative oxygenation.<sup>[a]</sup>

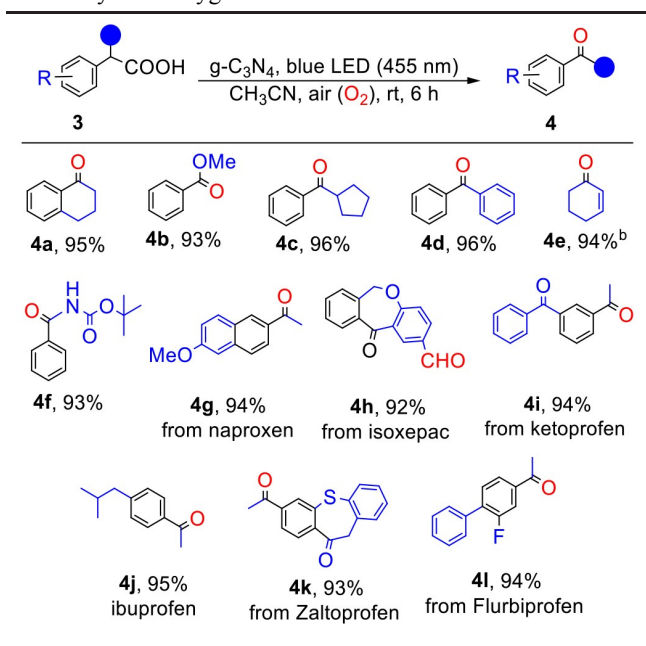


<sup>[a]</sup> Reaction conditions: **1** (0.5 mmol), g-C<sub>3</sub>N<sub>4</sub> (5 mg), CH<sub>3</sub>CN (3 mL), blue LED (455 nm), rt, atm. air, 6 h. Yields after isolation.

<sup>[b]</sup> GC-MS yield.

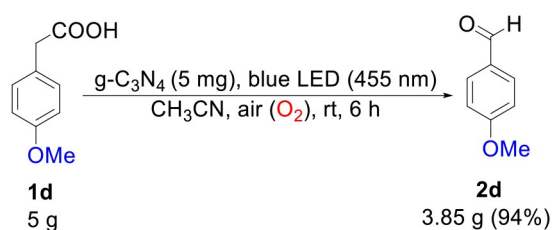
an external oxygen source in the reaction (Scheme 3a). An H<sub>2</sub><sup>18</sup>O experiment was performed to confirm the source of oxygen, the <sup>18</sup>O labelled product was not detected (Scheme 3b). When benzoquinone (2 equiv.) was added as a quencher to confirm the formation of the superoxide radical anion, no **2d** was detected (Scheme 3c). When sodium azide (2 equiv.) was added to the reaction mixture, no significant drop in the

**Table 3.** Substrates scope of secondary carboxylic acids for decarboxylative oxygenation.<sup>[a]</sup>



<sup>[a]</sup> Reaction conditions: **3** (0.5 mmol),  $g\text{-C}_3\text{N}_4$  (5 mg),  $\text{CH}_3\text{CN}$  (3 mL), blue LED (455 nm), rt, atm. air, 6 h. Yields after isolation.

<sup>[b]</sup> GC-MS yield.



**Scheme 2.** Gram-scale reaction of 4-methoxybenzaldehyde.

product yield was observed, which excludes the involvement of singlet oxygen in the reaction mechanism (Scheme 3d). Additionally, no reaction was observed when the radical scavenger TEMPO was employed, and a benzyl-TEMPO (**M**) trapping product was confirmed from ESI-MS, indicating that the reaction proceeds via radical pathways (Scheme 3e and SI, Figure S6). EPR-spectral analysis in acetonitrile solution with 4-methoxy phenylacetic acid and DMPO confirms the presence of DMPO-benzyl radical (Figure 4).

In agreement with the literature and based on the observations of the control experiments, we propose the catalytic cycle as outlined in Scheme 4. Under visible light irradiation,  $g\text{-C}_3\text{N}_4$  gets excited to result in an efficient separation of photogenerated electron-hole pairs.<sup>[31,34,36]</sup> The conduction band electrons reduce the

**Table 4.** Photo-oxidative cleavage of olefins.<sup>[a]</sup>

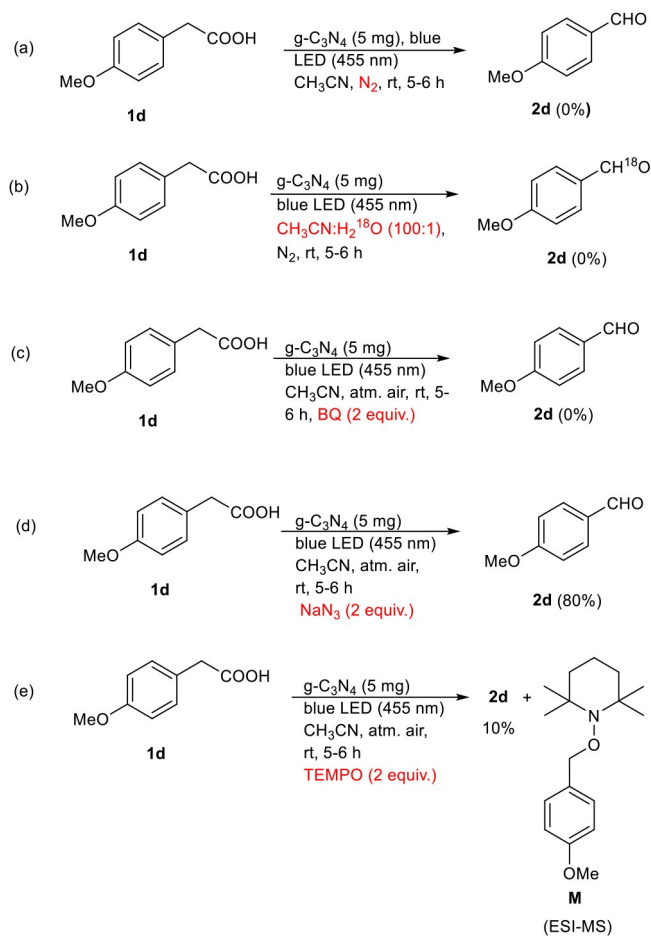
Reaction scheme showing the conversion of olefin **5** to aldehyde/ketone **6** using  $g\text{-C}_3\text{N}_4$  (5 mg), blue LED (455 nm),  $\text{CH}_3\text{CN}$ , air ( $\text{O}_2$ ), rt, 6 h.

Entry	Substrate	Product	Yield (%)
1	Ph-CH=CH <sub>2</sub>	Ph-CHO	96 <sup>b</sup>
2	Ph-CH=CH-Ph	Ph-CHO	97 <sup>b</sup>
3	Ph-CH=CH-Ph	Ph-CHO	90 <sup>b</sup>
4	Ph-C(=CH <sub>2</sub> )-CH <sub>3</sub>	Ph-CO-CH <sub>3</sub>	96 <sup>b</sup>
5	Ph-C(=CH-Ph)-CH <sub>3</sub>	Ph-CO-Ph	98
6	2-vinylpyridine	2-pyridyl-CHO	92 <sup>b</sup>
7	2-vinylthiophene	2-thiophenyl-CHO	90 <sup>b</sup>
8	2-vinylfuran	2-furyl-CHO	90 <sup>b</sup>
9	4-methoxy-1-butene	4-methoxybenzaldehyde	95
10	4-methyl-1-butene	4-methylbenzaldehyde	90
11	4-(trimethylsilyloxy)-1-butene	4-(trimethylsilyloxy)benzaldehyde	94
12	4-nitro-1-butene	4-nitrobenzaldehyde	92
13	4-bromo-1-butene	4-bromobenzaldehyde	90
14	4-(tert-butyl)-1-butene	4-(tert-butyl)benzaldehyde	89
15	1-(2-naphthyl)-1-butene	2-naphthyl-CHO	90

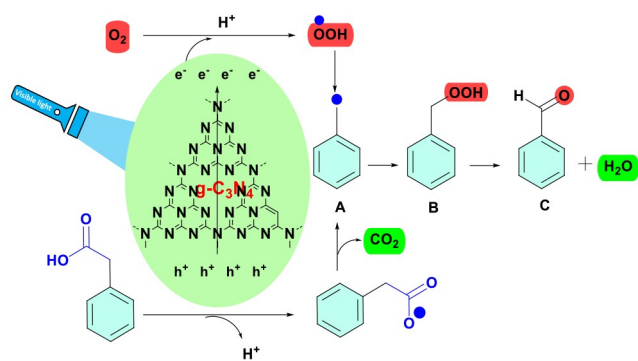
<sup>[a]</sup> Reaction conditions: **5** (0.5 mmol),  $g\text{-C}_3\text{N}_4$  (5 mg),  $\text{CH}_3\text{CN}$  (3 mL), blue LED (455 nm), rt, atm. air, 6 h. Yields after isolation.

<sup>[b]</sup> GC yield.

dioxygen and produce superoxide radicals. The photo-generated hole of  $g\text{-C}_3\text{N}_4$  further undergoes single electron transfer (SET) with the phenylacetic acid to afford benzylic radical **A**. **A** can be trapped by the peroxide radical  $\bullet\text{OOH}$  from superoxide anions to generate intermediates **B**, which undergoes water elimination to give rise to aldehyde or ketone **C**.



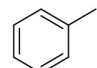
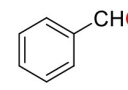
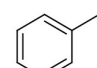
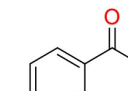
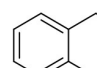
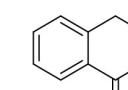
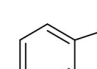
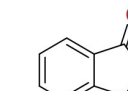
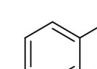
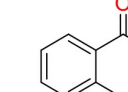
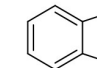
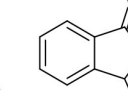
**Scheme 3.** Control experiments for decarboxylative oxygenations. Conditions: **1d** (0.1 mmol),  $g\text{-C}_3\text{N}_4$  (5 mg),  $\text{CH}_3\text{CN}$  (3 mL), blue light (455 nm), rt.



**Scheme 4.** Plausible Mechanism based on experimental investigation.

In conclusion, we have developed an entirely metal-free heterogeneous photocatalytic system for the aerobic oxidation of structurally diverse  $sp^3$  (C–H) bonds of aryl acetic acids, hetero(aromatic) acetic

**Table 5.** C ( $sp^3$ )–H bond oxidation of alkylarenes.<sup>[a]</sup>

$\text{R}^1\text{CH}_2\text{CH}_2\text{R}^2 \xrightarrow[\text{CH}_3\text{CN, air (O}_2\text{), rt, 6 h}]{g\text{-C}_3\text{N}_4 \text{ (5 mg), blue LED (455 nm)}} \text{R}^1\text{CH}_2\text{C(=O)R}^2$			
7	8		
Entry	Substrate	Product	Yield (%)
1.			80 <sup>b</sup>
2.			96 <sup>b</sup>
3.			89
4.			91
5.			97
6.			98

<sup>[a]</sup> Reaction conditions: **5** (0.5 mmol),  $g\text{-C}_3\text{N}_4$  (5 mg),  $\text{CH}_3\text{CN}$  (3 mL), blue LED (455 nm), rt, atm. air, 6 h. Yields after isolation.

<sup>[b]</sup> GC yield.

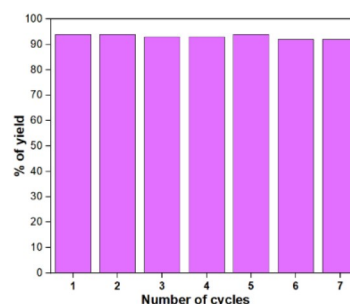


**Figure 2.** Catalyst recycling profile of  $g\text{-C}_3\text{N}_4$  after 7 cycles

acids, cyclohex-1-ene-2-carboxylic acid, 2-(4-((*tert*-Butoxycarbonyl)amino)phenyl)acetic acid, *tert*-Butyl (4-formylphenyl)carbamate, alkenes and alkyl arene

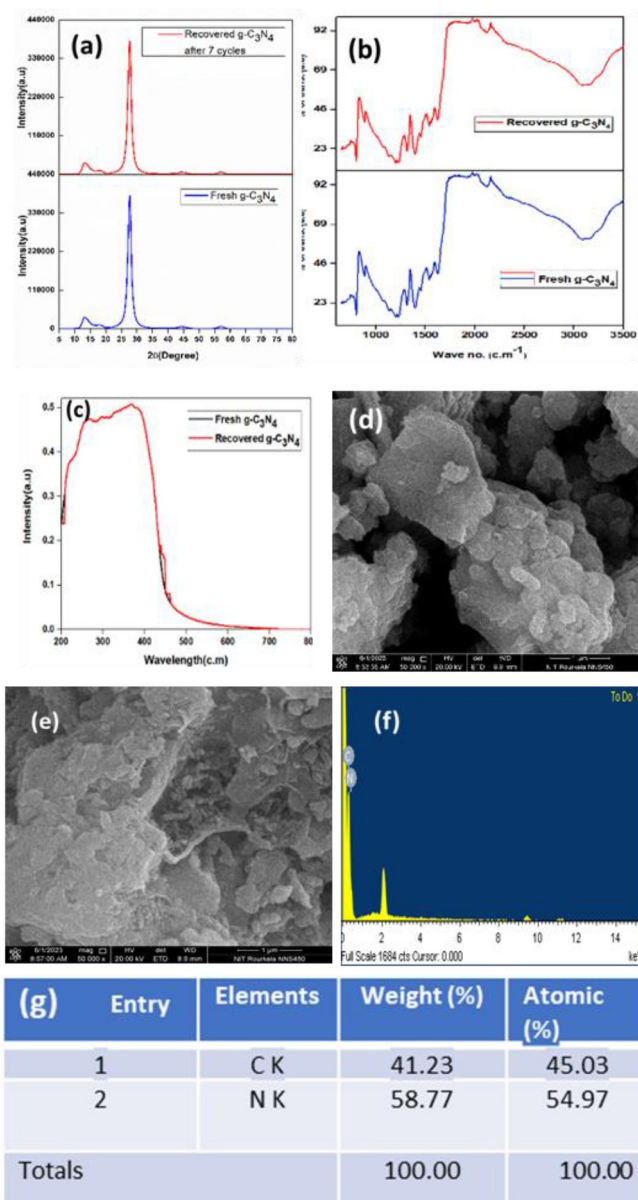


**Figure 3.** (a) XRD pattern, (b) IR, (c) UV-vis diffuse reflectance spectra (UV-vis DRS) of fresh  $g\text{-C}_3\text{N}_4$  and recovered  $g\text{-C}_3\text{N}_4$  after 7 cycles, (d) and (e) FESEM images of fresh and recovered  $g\text{-C}_3\text{N}_4$  after 7 cycles, (f) EDS image and (g) Surface atomic ratios of all elements measured by EDS of fresh  $g\text{-C}_3\text{N}_4$ .

with  $\text{O}_2$  as the green oxidant. This protocol employs readily accessible  $g\text{-C}_3\text{N}_4$  as a visible-light-driven photocatalyst, featuring low cost and recyclability, comparing well concerning oxidant (air instead of oxygen), additives (no base needed), and reaction time to mesoporous graphitic nitride (mpg-CN). It allows for the generation of a broad range of synthetically and biologically valuable aldehydes, ketones, and amides from readily accessible acids under mild conditions.

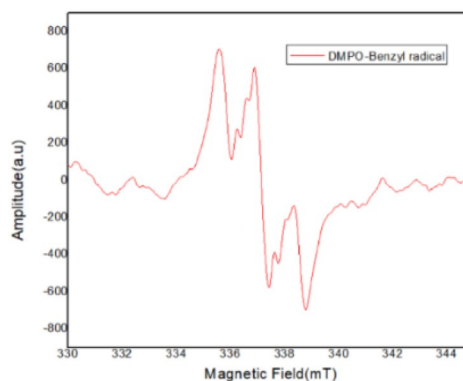


**Figure 4.** Electron spin resonance spectroscopy study.

## Experimental Section

### General Procedure for the Decarboxylative Oxidation of Carboxylic Acids by $g\text{-C}_3\text{N}_4$ under the Irradiation of Blue LED (455 nm)

A 5 mL oven-dried glass vial was charged with corresponding carboxylic acids (1 mmol, 1 equiv.), 3 mL dry  $\text{CH}_3\text{CN}$  and stirred vigorously to solubilize the solid compound. After that, 5 mg of  $g\text{-C}_3\text{N}_4$  was added to the reaction vessel and stirred for 5 h open to air under the irradiation of 0.9 W blue LED (450 nm). The temperature of 25–30 °C was maintained with the help of water circulation through the stir plate in case of 0.9 W blue LED and fan cooling in case of 1 W blue LED. The completion of the reaction was confirmed by thin layer chromatography and the reaction mixture was centrifuged to recover the catalyst. Then, evaporation of the organic solvent followed by column chromatography with silica and elution with appropriate petroleum ether/ $\text{CH}_3\text{COOC}_2\text{H}_5$  solvent mixture afforded the corresponding aldehyde and ketone.

### Procedure for the 30 mmol Scale Oxidation of 4-methoxy Phenylacetic Acid

A 100 mL round bottom flask was charged with 4-methoxy phenylacetic acid (5 g, 30 mmol, 1 equiv.). Subsequently,  $g\text{-C}_3\text{N}_4$  (5 mg) and 25 mL dry  $\text{CH}_3\text{CN}$  were added to the solution. After continuous stirring for 5 h under the irradiation of 1 W blue LED with fan cooling, the reaction mixture was monitored by TLC. Upon completion of the reaction, the crude mixture was centrifuged to separate the catalyst for the recycling experiment. The organic layer is concentrated over reduced pressure. The crude product was then purified by column chromatography using a 10%  $\text{CH}_3\text{COOC}_2\text{H}_5$ /petroleum ether solvent mixture.

3.85 g (94%) of 4-methoxy benzaldehyde was collected after column chromatography.

## Acknowledgements

We sincerely acknowledge the Department of Science and Technology (DST), Govt. of India (Grant Nos. EEQ/2020/000463 and TTR/2020/000015), CSIR, Govt. of India (Grant

No. 02(0443)/21/EMR-II), IGP- UGC (Grant No. F-1-7/2020(IC)), IITI/YFRSG/2022-23/1, DFG (TRR 325444632635-A2) and MoE-STARS (STARS-2/2023-1035). We thank SIC-IIT Indore for 500MHz NMR Facility, Department of Chemistry, IIT Indore for funding support and instrumental support. NIT Rourkela for instrumental facility and funding support. S.B. thanks CSIR for the Senior Research Fellowship. SB thanks UGC for the travel grant. Open Access funding enabled and organized by Projekt DEAL.

## References

- [1] N. L. Reed, T. P. Yoon, *Chem. Soc. Rev.* **2021**, *50*, 2954–2967.
- [2] M. Uygur, J. H. Kuhlmann, M. C. Pérez-Aguilar, D. G. Piekarski, O. García Mancheño, *Green Chem.* **2021**, *23*, 3392–3399.
- [3] C. Tang, X. Qiu, Z. Cheng, N. Jiao, *Chem. Soc. Rev.* **2021**, *50*, 8067–8101.
- [4] J. Zhang, J. Du, C. Zhang, K. Liu, F. Yu, Y. Yuan, B. Duan, R. Liu, *Org. Lett.* **2022**, *24*, 1152–1157.
- [5] F. Jiang, S. Liu, W. Zhao, H. Yu, L. Yan, Y. Wei, *Dalton Trans.* **2021**, *50*, 12413–12418.
- [6] J. Cheung, M. J. Rudolph, F. Burshteyn, M. S. Cassidy, E. N. Gary, J. Love, M. C. Franklin, J. J. Height, *J. Med. Chem.* **2012**, *4*.
- [7] S. Shirase, S. Tamaki, K. Shinohara, K. Hirose, H. Tsurugi, T. Satoh, K. Mashima, *J. Am. Chem. Soc.* **2020**, *142*, 5668–5675.
- [8] R. Guan, E. L. Bennett, Z. Huang, J. Xiao, *Green Chem.* **2022**, *24*, 2946–2952.
- [9] Y. Sakakibara, P. Cooper, K. Murakami, K. Itami, *Chem. Asian J.* **2018**, *13*, 2410–2413.
- [10] T. M. Faraggi, W. Li, D. W. C. MacMillan, *Isr. J. Chem.* **2020**, *60*, 410–415.
- [11] T. Rahman, G. Borah, P. K. Gogoi, *Catal. Lett.* **2020**, *150*, 2267–2272.
- [12] T. B. Mete, T. M. Khopade, R. G. Bhat, *Tetrahedron Lett.* **2017**, *58*, 2822–2825.
- [13] S. Farhadi, P. Zaringhadam, R. Z. Sahamieh, *Tetrahedron Lett.* **2006**, *47*, 1965–1968.
- [14] K. Gholam Reza, A. Roxana, *Chem. Res. Chin. Univ.* **2008**, *24*, 464–468.
- [15] S. Tangestaninejad, V. Mirkhani, *J. Chem. Res. Synop.* **1998**, 820–821.
- [16] M. Araghi, F. Bokaei, *Polyhedron* **2013**, *53*, 15–19.
- [17] A. Reichle, H. Sterzel, P. Kreitmeier, R. Fayad, F. N. Castellano, J. Rehbein, O. Reiser, *Chem. Commun.* **2022**, *58*, 4456–4459.
- [18] S. Swaminathan, J. K. Bera, M. Chandra, *Angew. Chem. Int. Ed.* **2023**, *62*, e202215933.
- [19] Z. Huang, R. Guan, M. Shanmugam, E. L. Bennett, C. M. Robertson, A. Brookfield, E. J. L. McInnes, J. Xiao, *J. Am. Chem. Soc.* **2021**, *143*, 10005–10013.
- [20] P. S. Bailey, *Chem. Rev.* **1958**, *58*, 925–1010.
- [21] T. Liu, F. Xue, Z. Chen, Z. Cheng, W. Cao, B. Wang, W. Jin, Y. Xia, Y. Zhang, C. Liu, *J. Catal.* **2022**, *414*, 76–83.
- [22] A. Ruffoni, C. Hampton, M. Simonetti, D. Leonori, *Nature* **2022**, *610*, 81–86.
- [23] Y. Zhang, N. Hatami, N. S. Lange, E. Ronge, W. Schilling, C. Jooss, S. Das, *Green Chem.* **2020**, *22*, 4516–4522.
- [24] T. R. Ahammad, S. Z. Gomes, J. Sreekrishnan, *J. Chem. Technol. Biotechnol.* **2008**, *83*, 1163–1169.
- [25] A. Pokutsa, S. Tkach, A. Zaborovsky, P. Bloniarz, T. Paczeński, J. Muzart, *ACS Omega* **2020**, *5*, 7613–7626.
- [26] J. Wu, J. Chen, L. Wang, H. Zhu, R. Liu, G. Song, C. Feng, Y. Li, *Green Chem.* **2023**, *25*, 940–945.
- [27] Y. Wang, P. Li, J. Wang, Z. Liu, Y. Wang, Y. Lu, Y. Liu, L. Duan, W. Li, S. Sarina, H. Zhu, J. Liu, *Catal. Sci. Technol.* **2021**, *11*, 4429–4438.
- [28] V. Patel, A. Baskar, S. Tiburcius, B. Morrison, B. Mod, P. S. Tanwar, P. Kumar, A. Karakoti, G. Singh, A. Vinu, *Adv. Sens. Res.* **2023**, *2*, 2300024.
- [29] K. Murugesan, A. Sagadevan, L. Peng, O. Savateev, M. Rueping, *ACS Catal.* **2023**, *13*, 13414–13422.
- [30] Y. Wang, X. Wang, M. Antonietti, *Angew. Chem. Int. Ed.* **2012**, *51*, 68–89.
- [31] A. Alaghamdard, K. Ghandi, *Nanomaterials* **2022**, *12*, 294.
- [32] Y. Zheng, L. Lin, B. Wang, X. Wang, *Angew. Chem. Int. Ed.* **2015**, *54*, 12868–12884.
- [33] J. Wen, J. Xie, X. Chen, X. Li, *Appl. Surf. Sci.* **2017**, *391*, 72–123.
- [34] Y. Cai, Y. Tang, L. Fan, Q. Lefebvre, H. Hou, M. Rueping, *ACS Catal.* **2018**, *8*, 9471–9476.
- [35] W. J. Ong, L. L. Tan, Y. H. Ng, S. T. Yong, S. P. Chai, *Chem. Rev.* **2016**, *116*, 7159–7329.
- [36] X. Wang, S. Blechert, M. Antonietti, *ACS Catal.* **2012**, *2*, 1596–1606.
- [37] I. Ghosh, J. Khamrai, A. Savateev, N. Shlapakov, M. Antonietti, B. König, *Science* **2019**, *365*, 360–366.
- [38] M. Inagaki, T. Tsumura, T. Kinumoto, M. Toyoda, *Carbon* **2019**, *141*, 580–607.
- [39] S. Zhang, W. Yi, Y. Guo, R. Ai, Z. Yuan, B. Yang, J. Wang, *Nanoscale* **2021**, *13*, 3493–3499.